Electronic Supplementary Material (ESI) for CrystEngComm.
This journal is © The Royal Society of Chemistry 2024

Electronic Supplementary Information (ESI)

Rock-salt $Ti_{1-x}O$ → rutile TiO_{2-x} transformation twinning via pulsed laser deposition - Implications for the dense (hkl)-specific phase change and optoelectronic properties

Chang-Ning Huang, *,[a] Jian-Yu Chen, [a] Yu-Xuan Lin, [a] and Pouyan Shen [b]

[a] *Department of Chemical and Materials Engineering, Southern Taiwan University of Science and Technology, Tainan 710301, Taiwan, ROC*
[b] *Department of Materials and Optoelectronic Science, National Sun Yat-sen University, Kaohsiung 80424, Taiwan, ROC*

Results and discussion

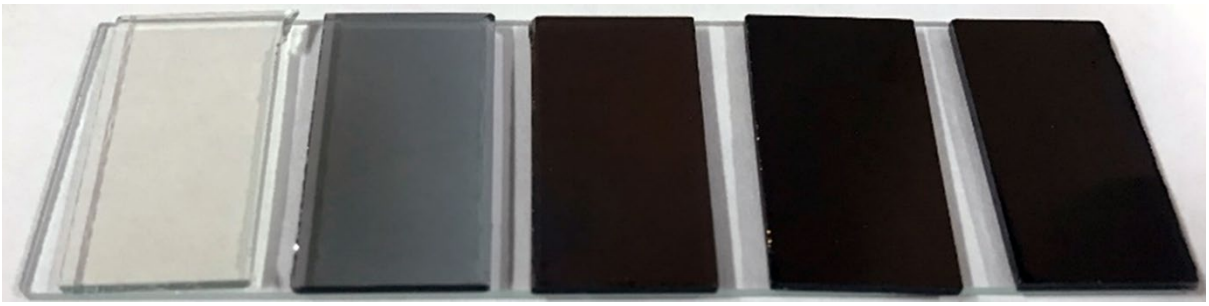

Fig. S1 Pristine FTO-coated silica glass substrate (whitish, far left) and such substrates overlain with gray to darkish films by PLA of rutile polycrystal target for 30 min in vacuum under 200, 400, 600, and 800 mJ/pulse, respectively from left to right.

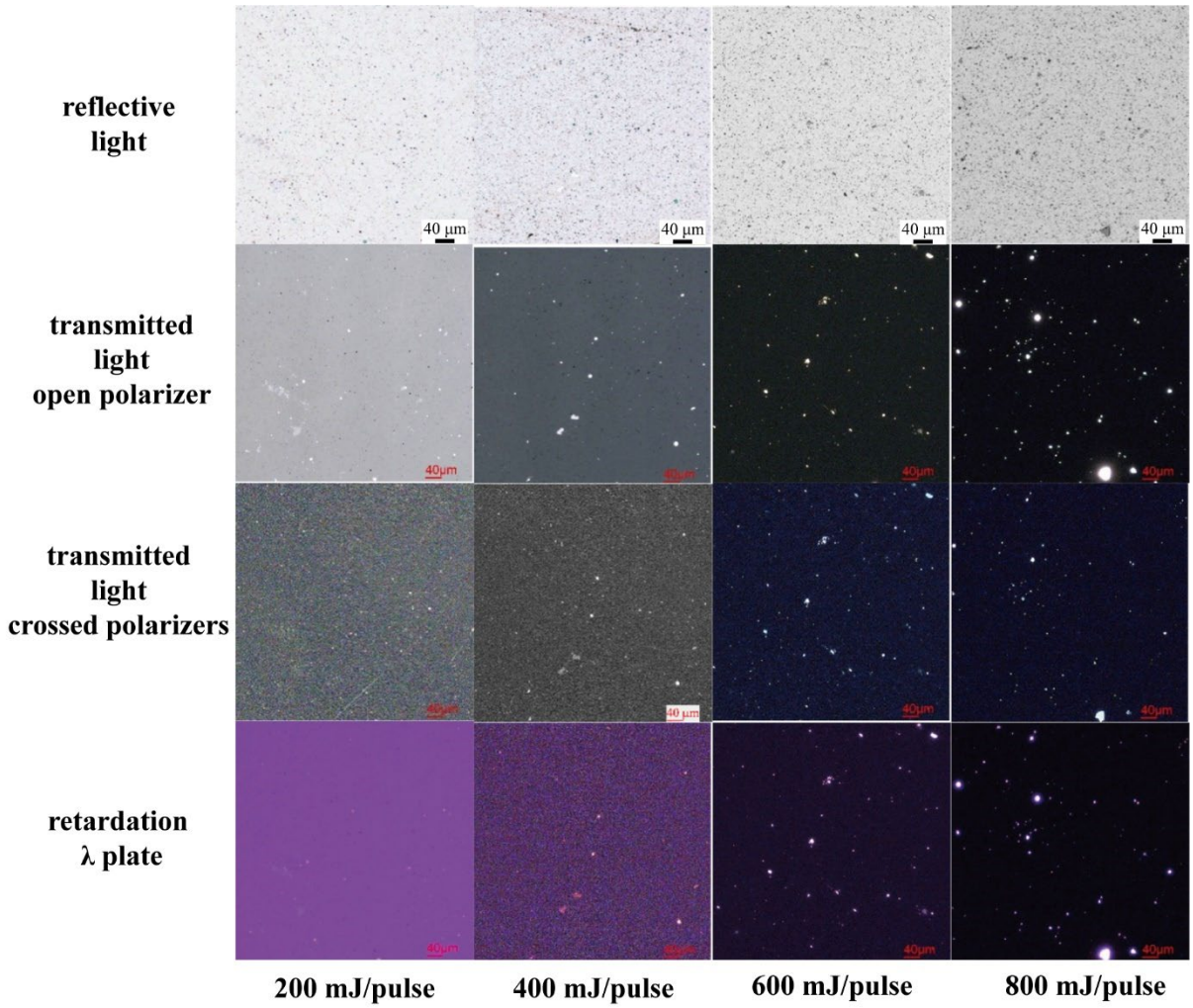

Fig. S2 Optical polarized microscopic images of the titanium oxide films deposited on FTO-coated silica glass slide under 200, 400, 600, and 800 mJ/pulse, respectively (from left to right) and in the top view under reflective light, transmitted light with open polarizer, crossed polarizers and further insertion of retardation λ plate (panels from top to bottom) showing micron-sized birefringent (bright) particles under crossed polarizers.

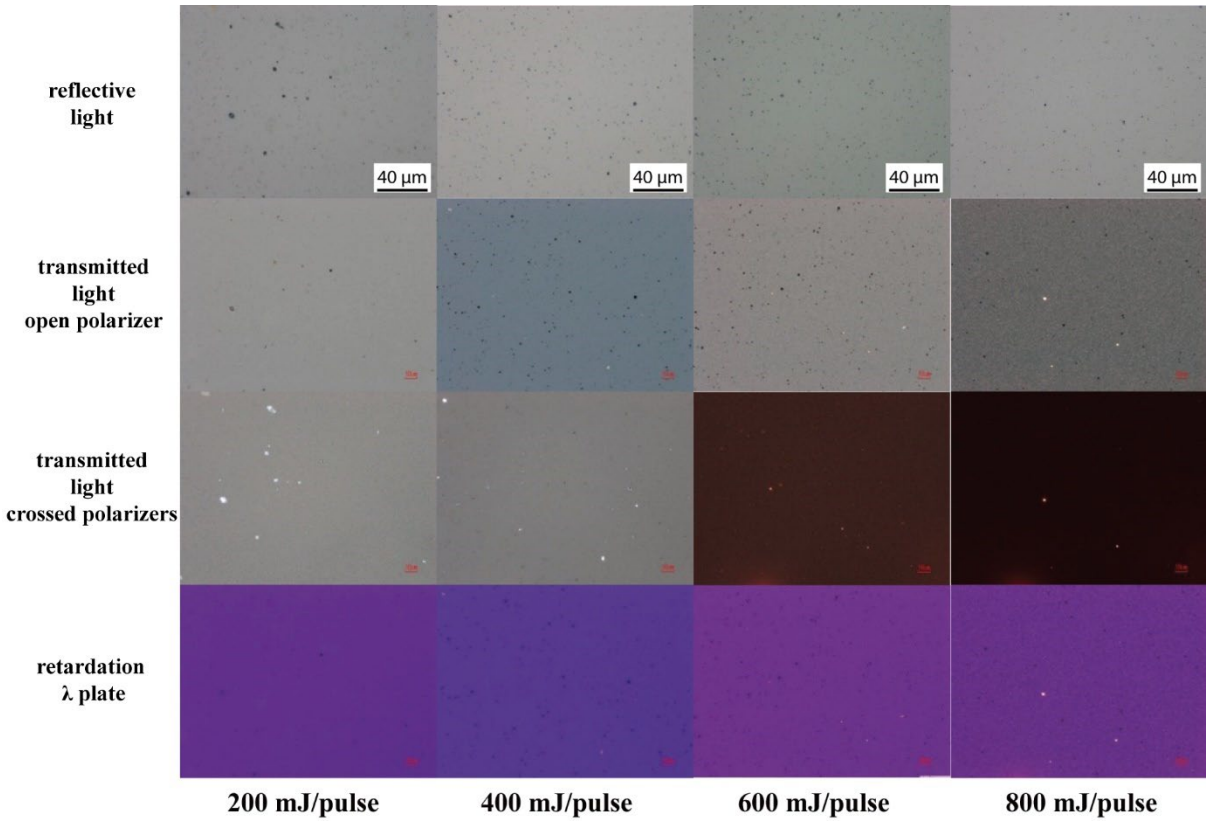

Fig. S3 Optical polarized microscopic images of the titanium oxide thin films as deposited on silica glass slides under 200, 400, 600, and 800 mJ/pulse, respectively (from left to right) and in the top view under reflective light, transmitted light with open polarizer, crossed polarizers and further insertion of retardation λ plate (panels from top to bottom) showing micron-sized birefringent (bright) particles under crossed polarizers.

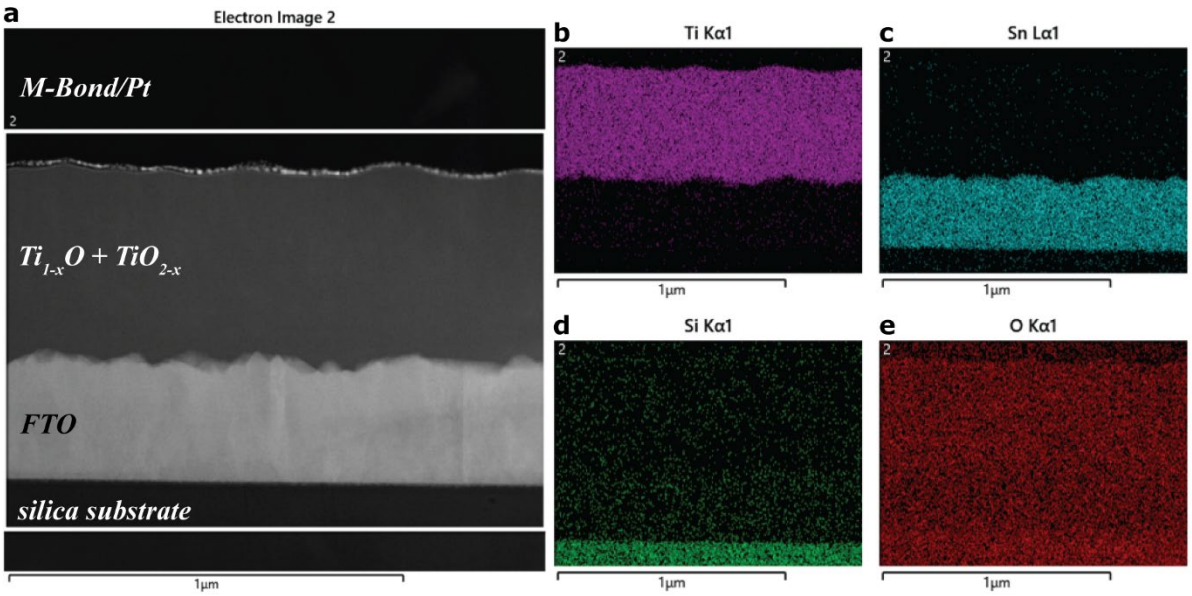

Fig. S4 (a) STEM-HAADF image and (b, c, d, e) Ti, Sn, Si, O X-ray mapping of the titanium oxide thin film deposited on FTO-coated silica glass under 800 mJ/pulse, with the interface viewed edge-on.

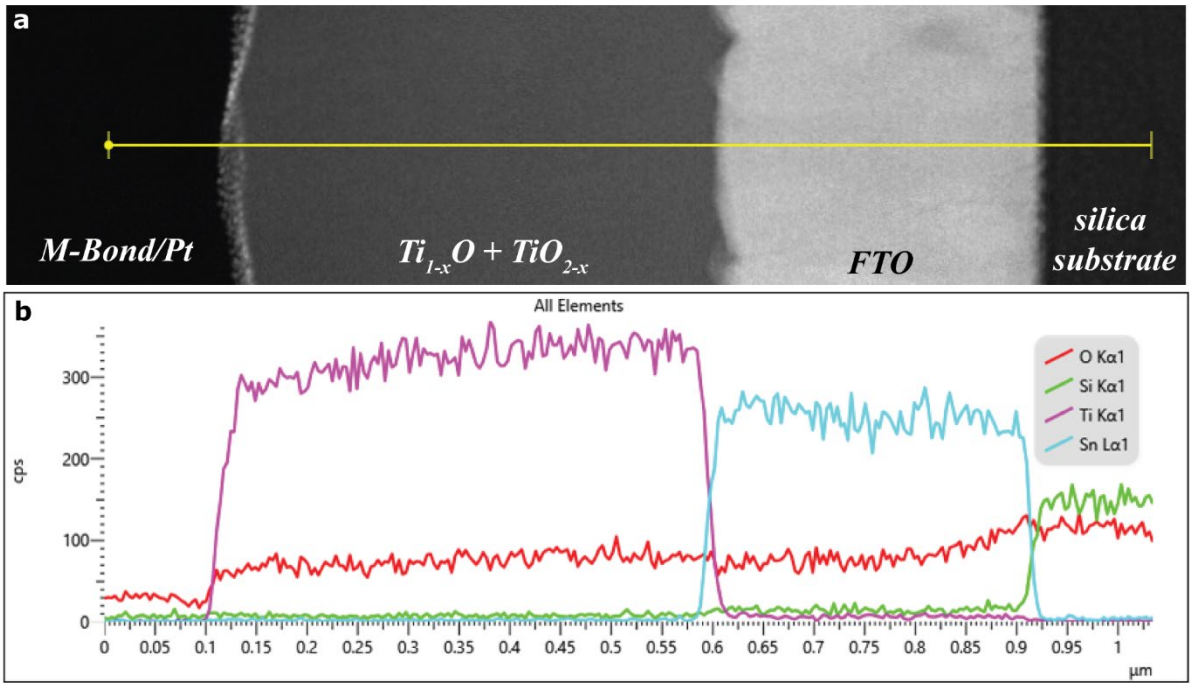

Fig. S5 (a) STEM-HAADF image and (b) Ti, Sn, Si, O X-ray line scanning across the R-$Ti_{1-x}O$+r-TiO_{2-x} predominant thin film deposited on FTO-coated silica glass under 800 mJ/pulse, with the interface viewed edge-on.

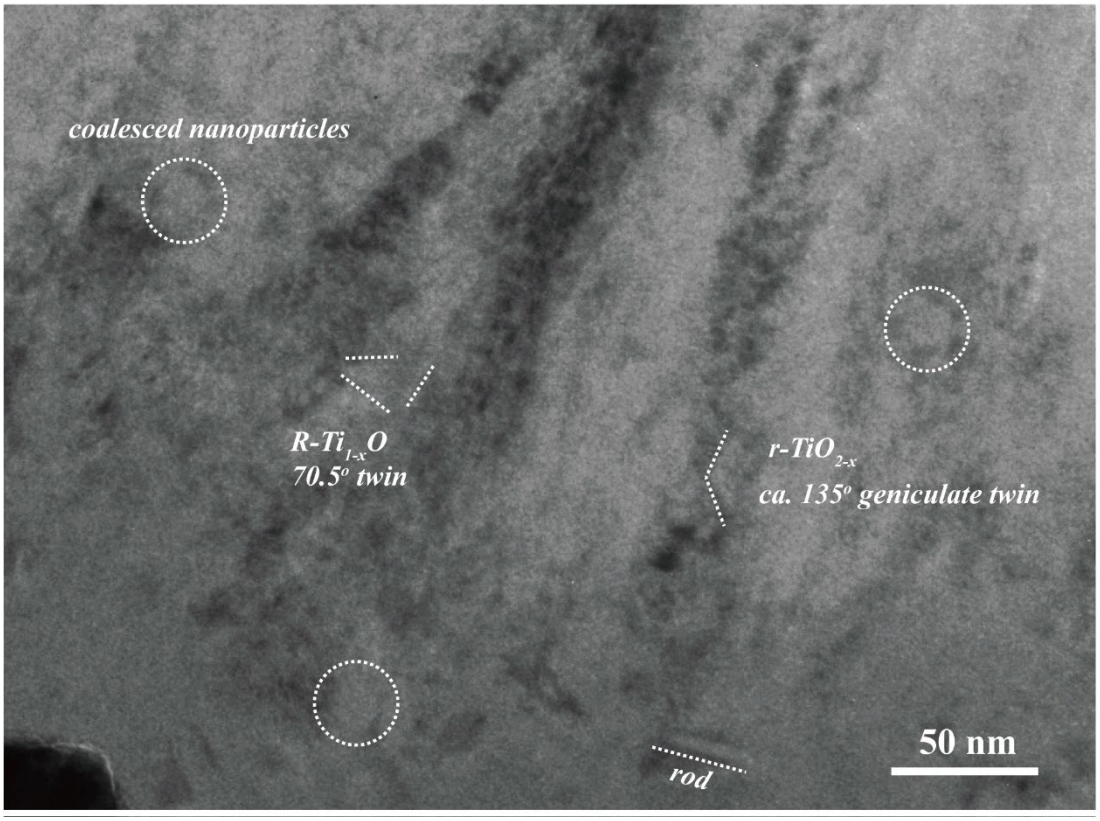

Fig. S6 TEM BFI magnified from Fig. 3a showing predominant R-$Ti_{1-x}O$ nanoparticles coalesced to form 70.5° twin boundary and minor r-TiO_{2-x} rods with geniculate 135° twin boundary in the film fabricated optimally at 600 mJ/pulse.

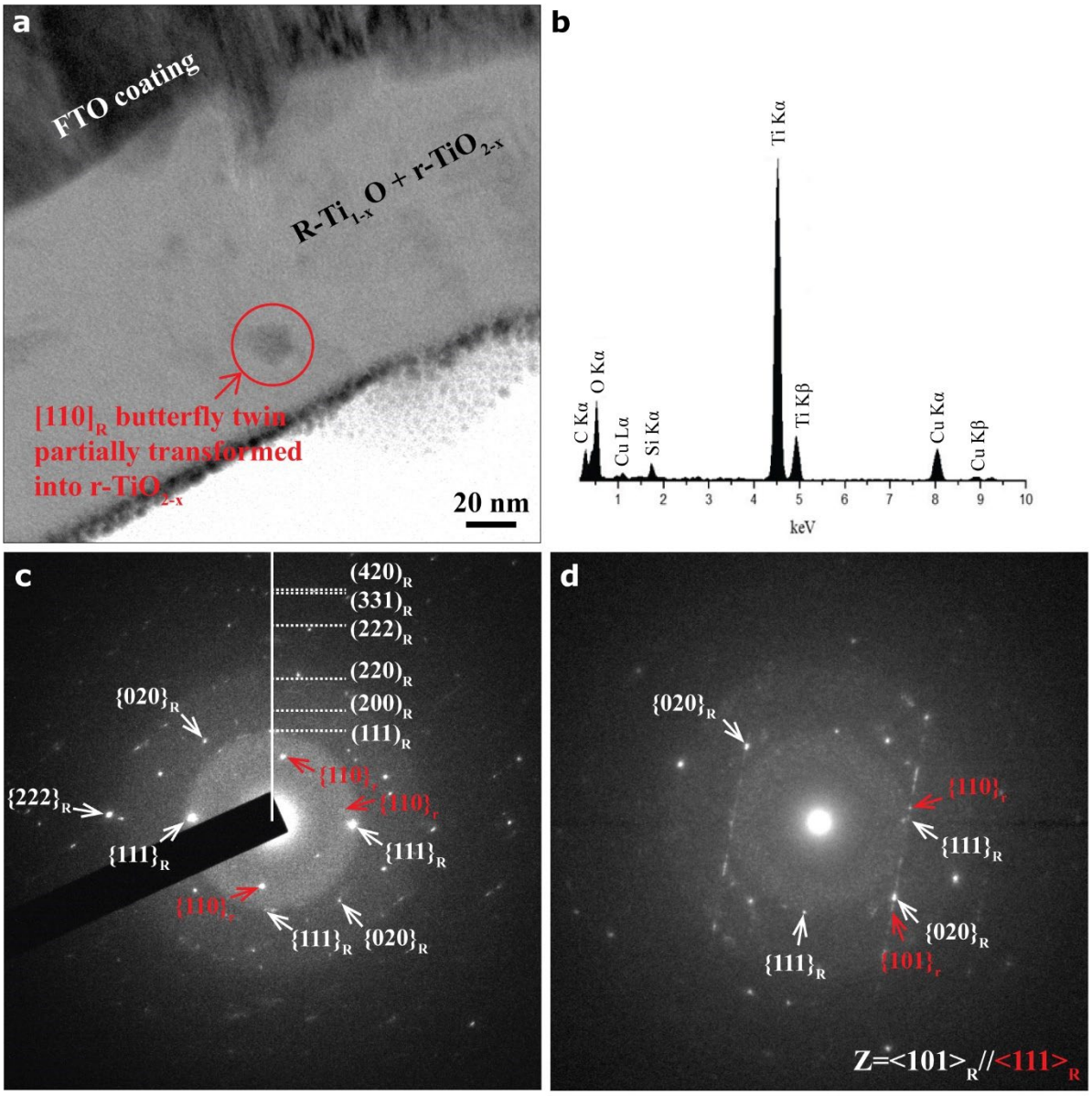

Fig. S7 TEM (a) BFI coupled with (b) EDX spectrum and (c) SAED pattern of the titania oxide thin film as deposited on FTO-coated silica glass by the PLA process under 200 mJ/pulse in vacuum showing diffuse scattering due to abundant amorphous phase and diffraction spots/rings due to the predominant R-$Ti_{1-x}O$ nanocondensates with occasional butterfly twin (circled) that underwent a partial transformation into r-TiO_{2-x} as indicated by the μμ diffraction (d). Note that the R-$Ti_{1-x}O$ butterfly twin was partially transformed into the r-TiO_{2-x} twin with characteristic diffractions and double diffractions according to lattice image and IFFT in the exact $[101]_R$ zone axis after slight tilting of the FIB section (cf. Fig. 6). The C, Si, and Cu counts in the EDX spectrum were from carbon-coated collodion film or M-bond, silica substrate, and TEM copper grid, respectively.

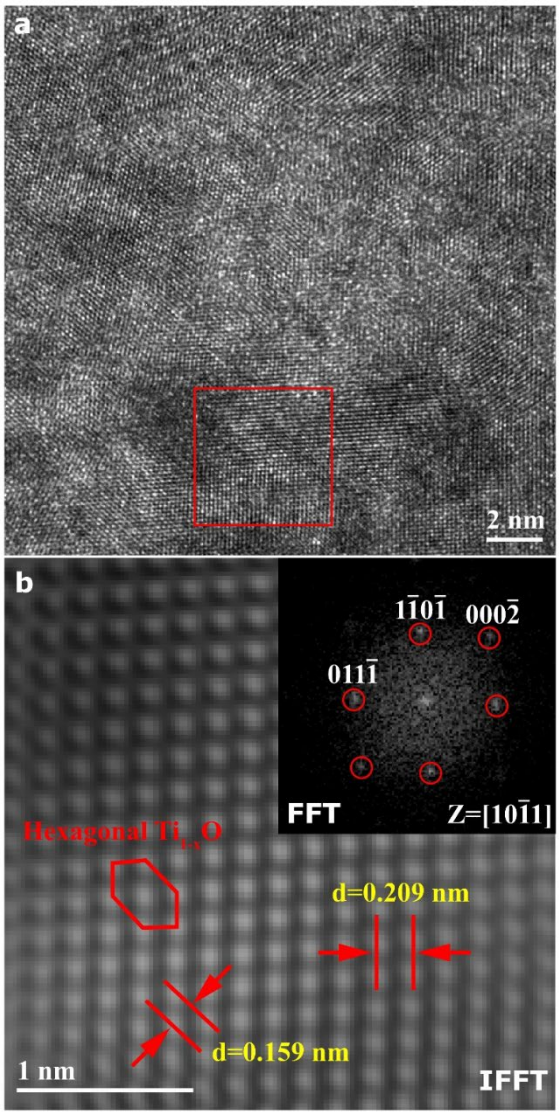

Fig. S8 TEM (a) lattice image (b) FFT (inset) and IFFT image from the square region of interest showing minor hexagonal $Ti_{1-x}O$ nanocondensate which survived in the film as deposited on FTO-coated silica glass by the PLA process under 600 mJ/pulse in vacuum.

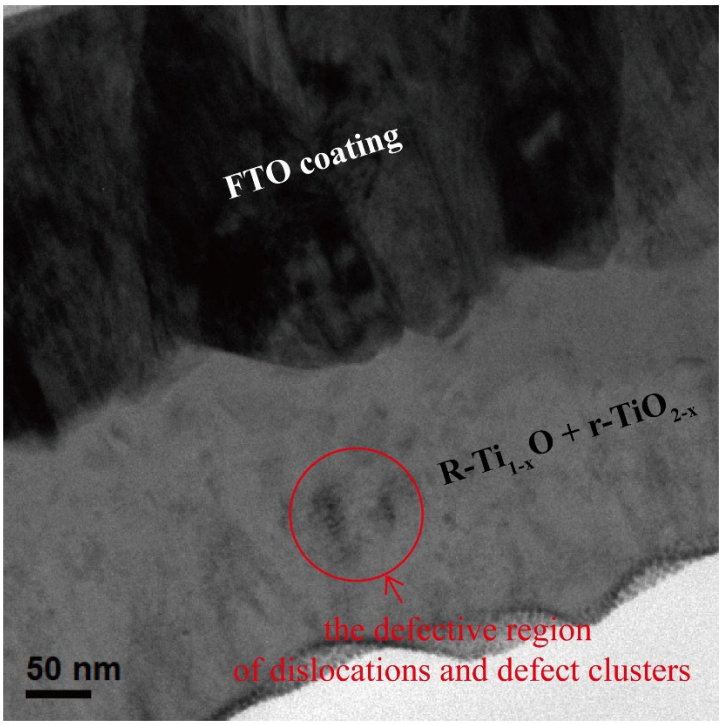

Fig. S9 Low-magnification TEM BFI of Fig. 5 showing the defective region in the titanium oxide thin film as deposited on FTO-coated silica glass by the PLA process under 200 mJ/pulse in vacuum.

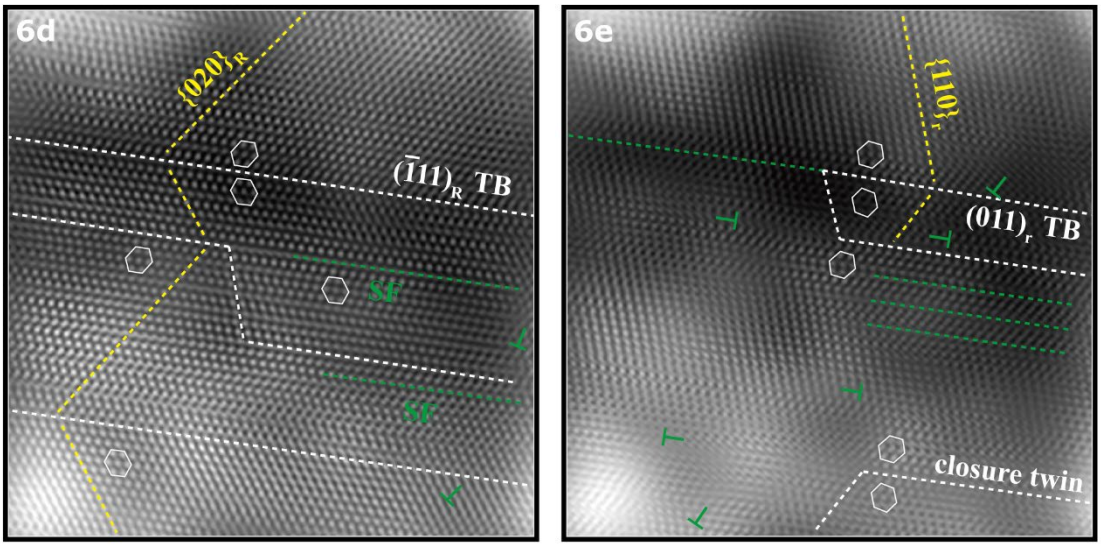

Fig. S10 Magnified Fig. 6d and 6e showing atomic plane (yellow dotted line), twin boundary (TB, white dashed line), stacking fault (SF, green dashed line), and dislocation (green T) of R-$Ti_{1-x}O$ and r-TiO_{2-x}, respectively, which occurred as intimate intergrowths in the composite twin bicrystal after the R → r partial transformation with accompanying polysynthetic deformation twin and closure twin for strain relaxation.

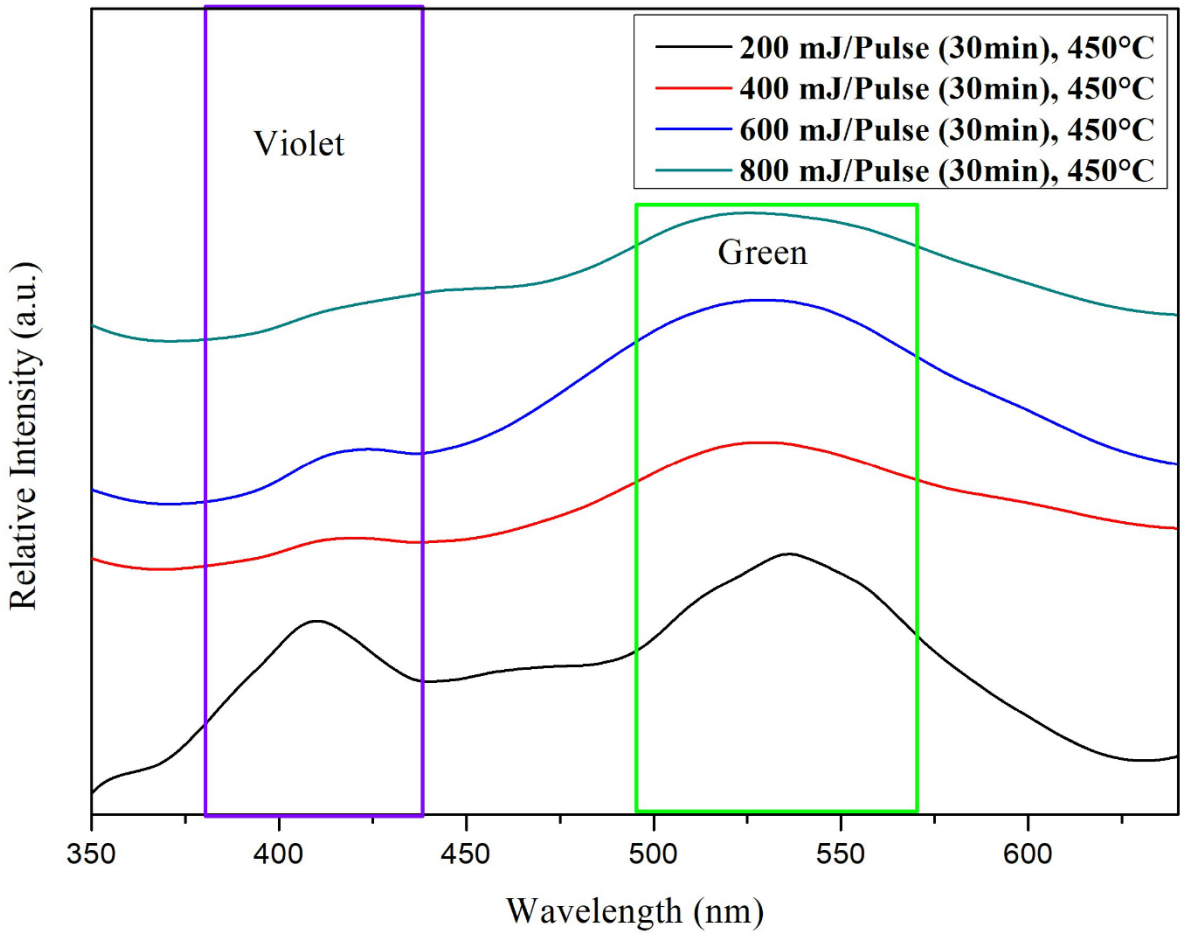

Fig. S11 PL spectra of the R-$Ti_{1-x}O$+r-TiO_{2-x} predominant thin film as deposited on FTO-coated silica glass by the PLA process in vacuum under a specified laser pulse energy of 200, 400, 600, and 800mJ/pulse, respectively followed by annealing at 450°C for 5 h in air.

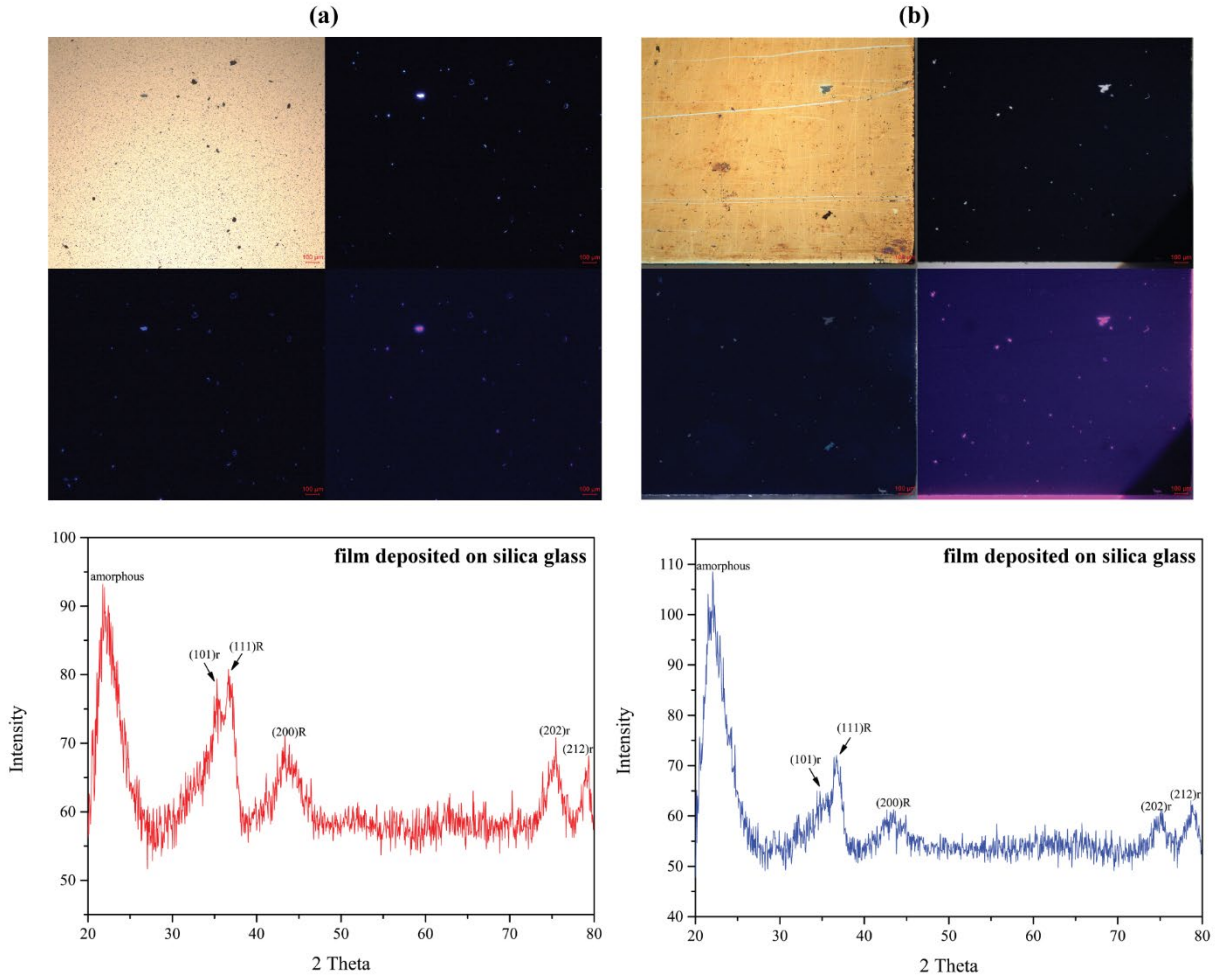

Fig. S12 Polarized optical microscopic (POM) images coupled with XRD trace of the titanium oxide thin films deposited on silica glass slides under 600mJ/pulse followed by (a) ambient dwelling for more than one year; (b) immersion in KOH solution for more than 12 hours and subjected to PEC measurement. The POM images are under reflective light (top left), transmitted light under open polarizer (top right), crossed polarizers (bottom left), and further insertion of retardation λ plate (bottom right) showing micron-sized birefringent (bright) particles under crossed polarizers.

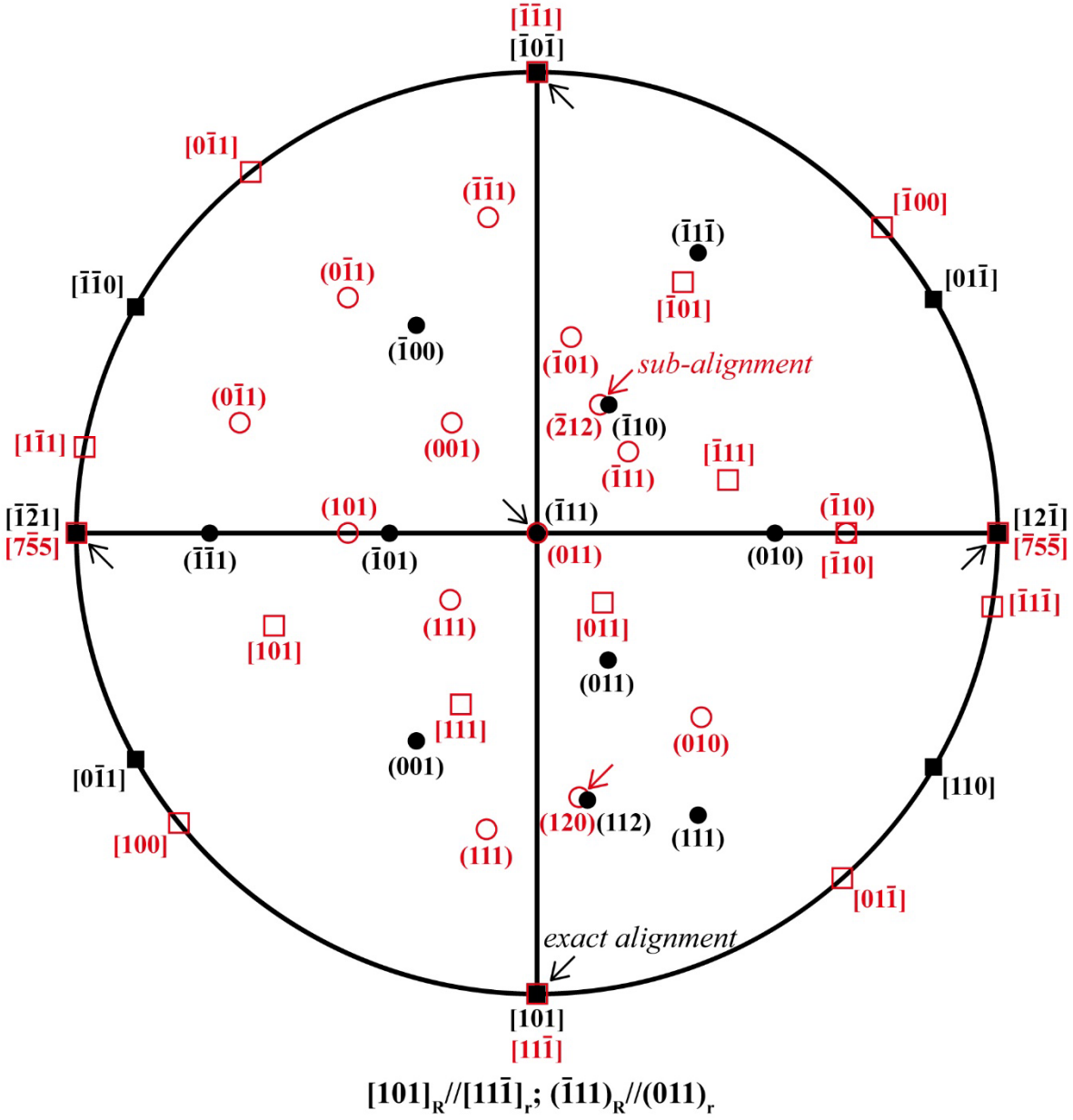

$[101]_R//[11\bar{1}]_r$; $(\bar{1}11)_R//(011)_r$

Fig. S13 Stereographic projection of the COR $[101]_R//[11\bar{1}]_r$; $(\bar{1}11)_R//(011)_r$ for R-$Ti_{1-x}O$ (black) and r-TiO_{2-x} (red) having the zone axis and plane normal denoted as square and circle, respectively.

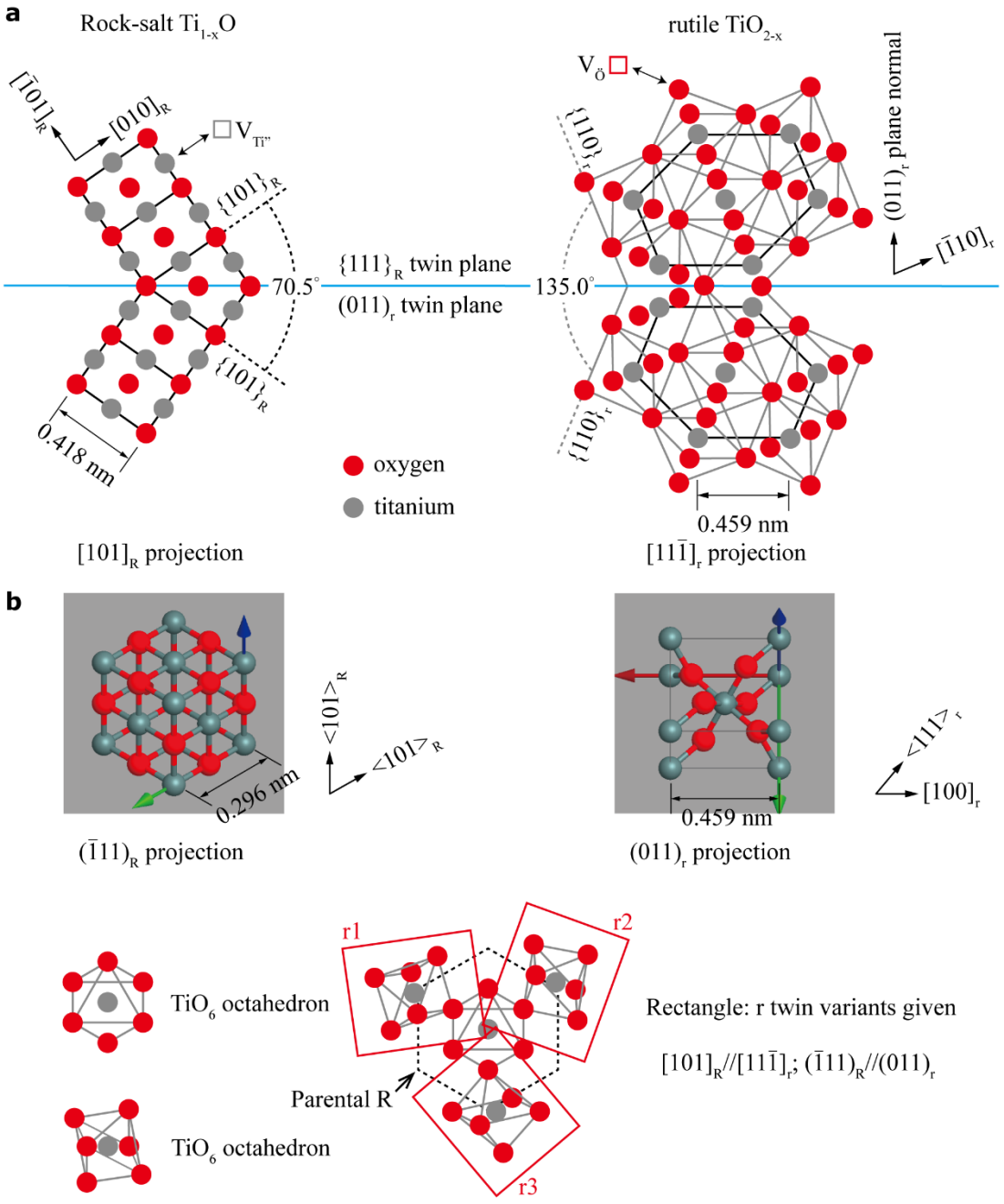

Fig. S14 Illustration of atoms disposition for the R → r transformation double twin boundary showing the projection direction and plane trace of the R and r lattices in perspective: (a) edge-on and (b) top view with topologically allowed three twin variants for the CSL (cf. Figure 12) involving considerable TiO_6 rotation given the COR $[101]_R//[11\bar{1}]_r$; $(\bar{1}11)_R//(011)_r$. Note the geniculate structure unit at $(\bar{1}11)_R$ twin boundary and $(011)_r$ twin boundary, presumably with O or Ti atoms merged from neighboring layers in (a) and the TiO_6 octahedra having face exactly and almost parallel to the dense $\{111\}_R$ and $(011)_r$ planes, respectively in (b).

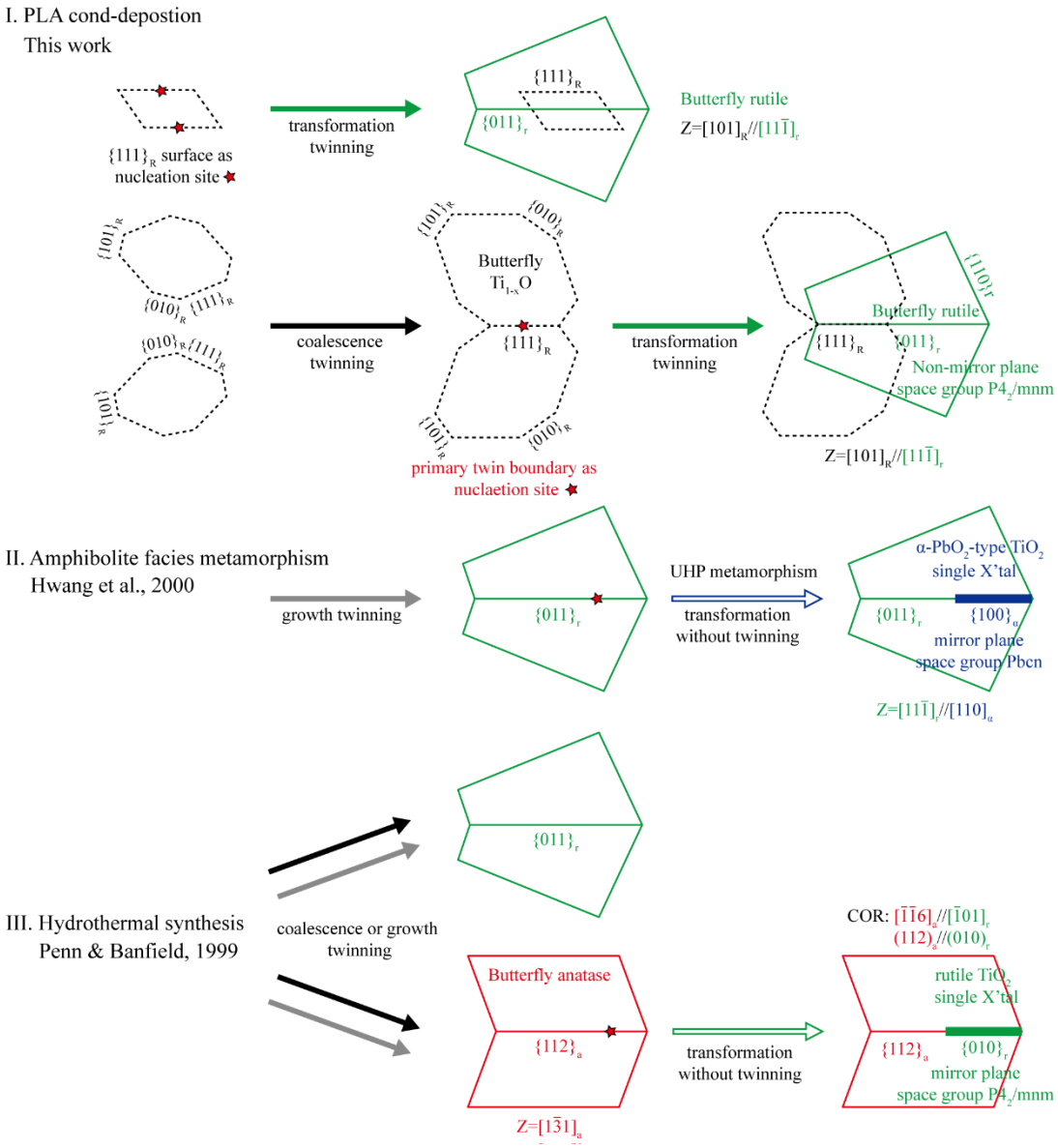

Fig. S15 Schematic drawing for the criterion of secondary butterfly-transformation twin, i.e. about the two daughter crystals sharing an atomic plane that happens to be a non-mirror plane such as the $(011)_r$ of rutile TiO_{2-x} by PLA condensation-deposition in this work in contrast to other documented cases (cf. text).